Robotica (2000) volume 18, pp. 325–336. Printed in the United Kingdom © 2000 Cambridge University Press

# Global adaptive partial state feedback tracking control of rigid-link flexible-joint robots*

W.E. Dixon, E. Zergeroglu, D.M. Dawson and M.W. Hannan

*Department of Electrical and Computer Engineering, Clemson University, Clemson, SC 29634-0915 (USA); e-mail: ddawson@eng.clemson.edu*

(Received in Final Form: August, 28, 1999)

**SUMMARY**

This paper presents a solution to the global adaptive partial state feedback control problem for rigid-link, flexible-joint (RLFJ) robots. The proposed tracking controller adapts for parametric uncertainty throughout the entire mechanical system while only requiring link and actuator position measurements. A nonlinear filter is employed to eliminate the need for link velocity measurements while a set of linear filters is utilized to eliminate the need for actuator velocity measurements. A backstepping control strategy is utilized to illustrate global asymptotic link position tracking. An output feedback controller that adapts for parametric uncertainty in the link dynamics of the robot manipulator is presented as an extension. Experimental results are provided as verification of the proposed controller.

KEYWORDS: Tracking control; Flexible-joint robots; Adaptive feedback; Backstepping strategy.

## 1. INTRODUCTION

Due to the elastic nature in which some gearing mechanisms (i.e. harmonic drives, belts, long shafts, etc.) transmit torque to the robot links, it is a widely accepted fact that the inclusion of joint flexibility in the dynamics for robot manipulators yields a more accurate model. In addition, the model for a rigid-link flexible-joint (RLFJ) robot includes uncertain parameters (i.e. inertia, friction, and stiffness effects); hence, controllers that can account for the parametric uncertainty seem highly desirable. Furthermore, from an implementation point of view, it is desirable that controllers be designed to require fewer measurements (i.e. due to the increased cost, complexity, and/or noise that additional sensors add to the system).

For some background on the design of controllers for rigid-link (RL) robot manipulators without link velocity measurements, the reader is referred to reference [1] and the references therein. With regard to the control of RLFJ robot manipulators, much of the previous research targeted setpoint control[2-4] although current research efforts have targeted the tracking control problem.[1,5-8] Specifically,[5] Qu proposed an input-output robust partial state feedback RLFJ tracking controller; however, link velocity measurements are required. Motivated by the desire to eliminate the dependence on velocity measurements, Nicosia and Tomei[6] proposed a semi-global exact knowledge (EMK) RLFJ tracking controller which only requires link position measurements. In reference [7], Lim et al. was able to employ a model-based observer approach to eliminate link and actuator velocity measurements to obtain semi-global exponential link position tracking for RLFJ robot manipulators. Moreover, Lim et al.,[8] also proposed an adaptive controller for the same problem given in reference [7]. Recently, solutions to the global output feedback tracking control problem were presented by Loria[9] and Zhang et al.[10] Specifically, the one-degree-of-freedom (DOF) robot manipulator control strategy, proposed in reference [9], provided motivation for the global adaptive and robust output feedback tracking controller designs for the n-DOF RL robot manipulator, proposed in references [10] and [11]. Based on the nonlinear link velocity filter structure,[10] and a model based observer for actuator position and velocity measurements, a global output feedback EMK link position tracking controller for RLFJ robot manipulators was proposed by Dixon et al.[1]

In this paper, we build on the previous work of [7] and [10] to design a global asymptotic link position tracking controller for RLFJ robot manipulators that only requires link and actuator position measurements and adapts parametric uncertainty throughout the entire mechanical system. Specifically, the proposed global adaptive partial state feedback tracking controller utilizes: i) a nonlinear link velocity filter, which is instrumental in eliminating link velocity measurements and maintaining the global stability result, ii) the output feedback control paradigm presented in [12] to eliminate actuator velocity measurements, and iii) the integrator backstepping technique to fuse the two aforementioned, dissimilar techniques together. This paper is organized as follows. Section 2 provides a mathematical model for an *n*-RFLJ, revolute, direct-drive robot and its associated properties. Section 3 presents the control objective and control design based on the RFLJ dynamics and Section 4 gives the main result of the paper. Section 5 presents an adaptive output feedback extension. Experimental verification of the proposed controller is provided in Section 6 and concluding remarks are given in Section 7.

* This work is supported in part by the U.S. National Science Foundation Grants DMI-9457967, CMS-9634796, ECS-9619785, DOE Grant DE-FG07-96ER14728, Gebze Institute for Advanced Technology, Gebze, Turkey, the Square D Corporation, and the Union Camp Corporation.

https://doi.org/10.1017/S0263574799002167 Published online by Cambridge University Press

## 2. ROBOT MANIPULATOR MODEL AND PROPERTIES

The mathematical model for an *n*-RFLJ, revolute, direct-drive robot is given by the following expression[13,14]

$$\underbrace{M(q)\ddot{q} + V_m(q, \dot{q})\dot{q} + G(q) + F_d\dot{q} = K_m(q_m - q)}_{\text{Robot Link Dynamics}} \quad (1)$$

$$\underbrace{J\ddot{q}_m + B\dot{q}_m + K_m(q_m - q) = u}_{\text{Robot Actuator Dynamics}}$$

where $q(t)$, $\dot{q}(t)$, $\ddot{q}(t) \in \Re^n$ denote link position, velocity, and acceleration, respectively, $q_m(t)$, $\dot{q}_m(t)$, $\ddot{q}_m(t) \in \Re^n$ denote joint position, velocity, and acceleration, respectively, $M(q) \in \Re^{n\times n}$ represents the link inertia effects, $V_m(q, \dot{q}) \in \Re^{n\times n}$ represents the centripetal-Coriolis effects, $G(q) \in \Re^n$ denotes gravity terms, $F_d$, $K_m$, $J$, $B \in \Re^{n\times n}$ are constant, diagonal, positive-definite matrices that represent link viscous friction, actuator flexibility, actuator inertia, and actuator viscous friction, respectively, and $u(t) \in \Re^n$ denotes the control torque input.

The dynamic equations of (1), exhibit the following properties[10,15] which are utilized in the subsequent controller development and analysis.

**Property 1:** $M(q)$ is a symmetric, positive-definite matrix, satisfying the following inequalities

$$m_1\|\xi\|^2 \le \xi^T M(q)\xi \le m_2\|\xi\|^2 \quad \forall \xi \in \Re^n \quad (2)$$

where $m_1$, $m_2$ are known positive constants, and $\|\cdot\|$ denotes the standard Euclidean norm.

**Property 2:** A skew symmetric relationship exists between the time derivative of the inertia matrix, $\dot{M}(q)$ and the centripetal-Coriolis matrix, $V_m(q, \dot{q})$. This useful relationship can be written in the following form

$$\xi^T\left(\frac{1}{2}\dot{M}(q) - V_m(q, \dot{q})\right)\xi = 0 \quad \forall \xi \in \Re^n. \quad (3)$$

**Property 3:** The dynamic equation of (1) can be linear parameterized as follows

$$Y_d(q_d, \dot{q}_d, \ddot{q}_d)\theta = M(q_d)\ddot{q}_d + V_m(q_d, \dot{q}_d)\dot{q}_d + G(q_d) + F_d\dot{q}_d \quad (4)$$

where known functions of the desired link position, velocity, and acceleration, $q_d(t)$, $\dot{q}_d(t)$, $\ddot{q}_d(t) \in \Re^n$, respectively are contained in the *desired* regression matrix $Y_d(q_d, \dot{q}_d, \ddot{q}_d) \in \Re^{n\times p}$, and $\theta \in \Re^p$ contains the constant unknown system parameters. As in reference [7] we assume that the left-hand side of (1) is second-order differentiable, and that $q_d(t)$ is selected to be fourth-order differentiable; hence, we know that $Y_d(q_d, \dot{q}_d, \ddot{q}_d)$ is second-order differentiable.

**Property 4:** The norm of the centripetal-Coriolis, and viscous friction terms of (1) can be upper bounded as follows

$$\|V_m(q, \dot{q})\|_{i\infty} \le \zeta_{c1}\|\dot{q}\|, \quad \|F_d\|_{i\infty} \le \zeta_f, \quad (5)$$

where $\zeta_{c1}$ and $\zeta_f$ are positive bounding constants, and $\|\cdot\|_{i\infty}$ denotes the induced infinity norm for a matrix.

**Property 5:** The centripetal-Coriolis matrix satisfies the following relationship

$$V_m(q, \xi)v = V_m(q, v)\xi \quad \forall \xi, v \in \Re^n. \quad (6)$$

**Property 6:** The vector function $Tanh(\cdot) \in \Re^n$, and the matrix functions $Cosh(\cdot) \in \Re^{n\times n}$ and $Sinh(\cdot) \in \Re^{n\times n}$ are defined as follows

$$\text{Tanh}(\xi) = [\tanh(\xi_1), \ldots, \tanh(\xi_n)]^T \quad (7)$$

$$\text{Cosh}(\xi) = diag\{\cosh(\xi_1), \ldots, \cosh(\xi_n)\} \quad (8)$$

and

$$\text{Sinh}(\xi) = diag\{\sinh(\xi_1), \ldots, \sinh(\xi_n)\} \quad (9)$$

where $\xi(t) = [\xi_1, \ldots, \xi_n]^T \in \Re^n$, and $diag\{\cdot\}$ denotes the standard diagonal matrix operation with only non-zero entries being on the diagonal. Based on these definitions, the following inequalities are true for all $\xi(t)$ and $v(t) \in \Re^n$

$$\frac{1}{2}\tanh^2(\|\xi\|) \le \ln(\cosh(\|\xi\|)) \le \sum_{i=1}^{n}\ln(\cosh(\xi_i)) \le \|\xi\|^2 \quad (10)$$

$$\tanh^2(\|\xi\|) \le \|\text{Tanh}(\xi)\|^2 = \text{Tanh}^T(\xi)\text{Tanh}(\xi)$$

$$\left|\cos\left(\sum_{i=1}^{n}\xi_i\right) - \cos\left(\sum_{i=1}^{n}\nu_i\right)\right| \le 8\sum_{i=1}^{n}|\tanh(\xi_i - \nu_i)|$$

$$\left|\sin\left(\sum_{i=1}^{n}\xi_i\right) - \sin\left(\sum_{i=1}^{n}\nu_i\right)\right| \le 8\sum_{i=1}^{n}|\tanh(\xi_i - \nu_i)| \quad (11)$$

where $\xi_i(t)$ and $v_i(t)$ are the $i$-th elements of the vectors $\xi(t)$ and $v(t)$, respectively, and $|\cdot|$ denotes the standard absolute value operation.

**Assumption 1:** The inertia, centripetal-Coriolis, and gravity terms of (1) can be upper bounded as shown by the following inequalities

$$\begin{aligned}\|M(\xi) - M(v)\|_{i\infty} &\le \zeta_m\|\text{Tanh}(\xi - v)\| \\ \|G(\xi) - G(v)\| &\le \zeta_g\|\text{Tanh}(\xi - v)\| \\ \|V_m(\xi, \dot{q}) - V_m(v, \dot{q})\|_{i\infty} &\le \zeta_{c2}\|\dot{q}\|\ \|\text{Tanh}(\xi - v)\|\end{aligned} \quad (12)$$

where $\zeta_m$, $\zeta_g$, and $\zeta_{c2}$ are positive bounding constants. Zhang et al.[10] illustrate how the bounds given in (12) hold for the six DOF Puma robot; hence, from a practical point of view, Assumption 1 resembles a property more than an assumption.

**Assumption 2:** We assume that known upper bounds for the unknown actuator parameter matrices $J$ and $K$ can be determined as follows

$$\lambda_{\max}\{J\} < \bar{J} \quad \lambda_{\max}\{K_m\} < \bar{K}_m \quad (13)$$

where $\bar{J}$, $\bar{K}_m \in \Re^1$ are known positive constants, and $\lambda_{\max}\{\cdot\}$ is used to denote the maximum eigenvalue.

## 3. CONTROL DEVELOPMENT

The control objective of this paper is to design a global adaptive partial state feedback tracking controller for the

https://doi.org/10.1017/S0263574799002167 Published online by Cambridge University Press

RLFJ robot modeled by (1). Specifically, the controller should force the links to asymptotically follow a desired trajectory despite the fact that the system parameters are uncertain and that link/actuator velocity measurements are unavailable. In order to quantify the control performance, the link position tracking error $e(t) \in \Re^n$ is defined as

$$e = q_d - q \tag{14}$$

where it is assumed that $q_d(t)$, and its first four time derivatives, are bounded functions of time. To quantify the effects of parametric uncertainty, we define a parameter estimation error vector $\tilde{\theta}(t) \in \Re^p$ as follows

$$\tilde{\theta} = \theta - \hat{\theta} \tag{15}$$

where $\hat{\theta}(t) \in \Re^p$ represents a dynamic estimate of $\theta(t) \in \Re^p$ defined in (4). Furthermore, motivated by the desire to compensate for the unknown parameter matrix $K_m$ given in (1) and the need to eliminate velocity measurements, we introduce an expanded regression matrix[16] $Y_{dx}(q_d, \dot{q}_d, \ddot{q}_d) \in \Re^{n \times np}$ and the parameter vector $\theta_x \in \Re^{np}$ based on $Y_d(q_d, \dot{q}_d, \ddot{q}_d)$ and $\theta$ as follows

$$Y_{dx} = Blockdiag[Y_{di}]_{i=1,\ldots,n} \tag{16}$$

and

$$\theta_x(t) = [\theta^T, \ldots, \theta^T]^T \tag{17}$$

where $Y_{di}(q_d, \dot{q}_d, \ddot{q}_d) \in \Re^{1 \times p}$ represents the $i$-th row vector of $Y_{di}(q_d, \dot{q}_d, \ddot{q}_d)$, and the notation *Blockdiag* $[\cdot]$ denotes a block diagonal matrix. We also define a new parameter matrix $K_{mx} \in \Re^{np \times np}$ as follows

$$K_{mx} = Blockdiag[K_{mi} I_p]_{i=1,\ldots,n} \tag{18}$$

where $K_{mi}$ represents the *i-th* diagonal element of $K_m$, and $I_p \in \Re^{p \times p}$ represents the standard identity matrix. Based on the definitions given in (16), (17), and (18), we can now rewrite the desired regression matrix in the following form

$$Y_d(q_d, \dot{q}_d, \ddot{q}_d)\theta = Y_{dx} K_{mx} K_{mx}^{-1} \theta_x = Y_{dx} K_{mx} \Phi_v \tag{19}$$

where the new parameter vector $\Phi_v \in \Re^{np}$ is defined as follows

$$\Phi_v = K_{mx}^{-1} \theta_x. \tag{20}$$

### *3.1. Control formulation*

In order to achieve the aforementioned control objective, we separate the control design into two stages. The first stage of the design is based on the link dynamics of (1), and the second stage is based on the actuator dynamics of (1). The global adaptive control design for the link dynamics entails implementing a link velocity independent control law that is comprised of a nonlinear link velocity filter. The control design for the actuator dynamics is developed through the use of a set of linear filters to eliminate the need for actuator velocity measurements.

### *3.2. Adaptive partial state feedback controller*

In this subsection we present the development of a nonlinear link velocity filter for the link dynamics. After the closed-loop error development, we present a partial Lyapunov-like stability analysis for the controller.

**3.2.1. Link velocity filter error system.** To facilitate the control development, we define a filtered tracking error-like term $\eta(t) \in \Re^n$ as follows

$$\eta = \dot{e} + \alpha_1 Tanh(e) + \alpha_2 Tanh(e_f) \tag{21}$$

where $\alpha_1, \alpha_2 \in \Re^1$ are positive constant filter gains, $Tanh(\cdot)$ and $e(t)$ are defined in (7) and (14) respectively, and $e_f(t) \in \Re^n$ is an auxiliary filter variable designed to have the following dynamic relationship

$$\dot{e}_f = -\alpha_3 Tanh(e_f) + \alpha_2 Tanh(e) - k Cosh^2(e_f)\eta, \tag{22}$$

where $k \in \Re^1$ is a positive constant control gain, $\alpha_3 \in \Re^1$ is a positive constant filter gain, and $Cosh(\cdot)$ is defined in (8). We also define a second auxiliary tracking error term $\eta_L(t) \in \Re^n$ as follows

$$\eta_L = q_{md} - q_m \tag{23}$$

in order to quantify how well the actual actuator position $q_m(t)$ tracks the desired actuator position $q_{md}(t) \in \Re^n$ (Note, the explicit expression for $q_{md}(t)$ is motivated by the subsequent stability analysis).

After taking the time derivative of (21), premultiplying both sides by $M(q)$, substituting (1), (21), and (22), adding/subtracting $K_m q_{md}$ and $Y_d\theta$ to the right-hand side of the resulting equation, and then utilizing *Property* 5, we obtain the following expression

$$\begin{aligned} M(q)\dot{\eta} = &- V_m(q, \dot{q})\eta - \alpha_2 k M(q)\eta + \chi + Y_d\theta \\ &+ K_m q - K_m q_m + K_m q_{md} - K_m q_{md} \end{aligned} \tag{24}$$

where $\chi(e, e_f, \eta, t) \in \Re^{n \times 1}$ is an auxiliary term defined as

$$\begin{aligned} \chi = &\alpha_1 M(q) Cosh^{-2}(e)(\eta - \alpha_1 Tanh(e) - \alpha_2 Tanh(e_f)) \\ &+ \alpha_2 M(q) Cosh^{-2}(e_f)(\alpha_2 Tanh(e) - \alpha_3 Tanh(e_f)) \\ &+ V_m(q, \dot{q}_d + \alpha_1 Tanh(e) + \alpha_2 Tanh(e_f))(\alpha_1 Tanh(e) \\ &+ \alpha_2 Tanh(e_f)) + M(q)\ddot{q}_d + V_m(q, \dot{q}_d)\dot{q}_d + G(q) + F_d\dot{q} \\ &+ V_m(q, \dot{q}_d)(\alpha_1 Tanh(e) + \alpha_2 Tanh(e_f)) \\ &- V_m(q, \eta)(\dot{q}_d + \alpha_1 Tanh(e) + \alpha_2 Tanh(e_f)) - Y_d\theta. \end{aligned} \tag{25}$$

**Remark 1** *Based on the properties of Tanh(·) defined in (7), and Cosh(·) defined in (8) utilizing Properties 1, 4, 5, Assumption 1, and the fact that $q_d(t)$ and its first four time derivatives are all bounded, it can be shown that*

$$\|\chi\| \le \zeta_1 \|x\| \tag{26}$$

*where $\zeta_1$ is a positive bounding constant, and $x(t) \in \Re^{3n}$ is defined as follows*

$$x = [\eta^T \quad Tanh^T(e) \quad Tanh^T(e_f)]^T. \tag{27}$$

Based on the open-loop error system given by (24) and the subsequent stability analysis, we design $q_{md}(t)$ in the following manner

$$q_{md} = Y_{dx}\hat{\Phi}_v + q - k\Psi Cosh^2(e_f)Tanh(e_f) + \Psi Tanh(e) \tag{28}$$

where $\Psi \in \Re^1$ is a positive constant control gain, the control gain $k \in \Re^1$ is defined as

$$k = \frac{1}{m_1}(1 + k_{n1}\zeta_1^2), \tag{29}$$

https://doi.org/10.1017/S0263574799002167 Published online by Cambridge University Press

$k_{n1} \in \Re^1$ is a positive constant nonlinear damping gain, and $\hat{\Phi}_v(t) \in \Re^{np}$ is an estimate for $\Phi_v$ of (20) via the following adaptive update law

$$\dot{\hat{\Phi}}_v = \Gamma Y_{dx}^T \eta \tag{30}$$

where $\Gamma \in \Re^{np \times np}$ is a positive definite, constant, diagonal, adaptation gain matrix. After substituting (19), (23), and (28) into (24), we obtain the final expression for the closed-loop dynamics for $\eta(t)$ as follows

$$\begin{aligned} M(q)\dot{\eta} = & -V_m(q,\dot{q})\eta - \alpha_2 k M(q)\eta + K_m Y_{dx}\tilde{\Phi}_v \\ & + k\Psi K_m Cosh^2(e_f) Tanh(e_f) \\ & - \Psi K_m Tanh(e) + K_m \eta_L + \chi \end{aligned} \tag{31}$$

where $\tilde{\Phi}_v(t) \in \Re^{np}$ is defined as

$$\tilde{\Phi}_v = \Phi_v - \hat{\Phi}_v. \tag{32}$$

**Remark 2** *Note that the adaptive update law given by (30) can be integrated by parts to obtain an implementable control signal for $\hat{\Phi}_v(t)$ that only depends on link position measurements (see [10]).*

**Remark 3** *Based on the structure of $\eta(t)$ defined in (21), it is clear that link velocity measurements are required for control implementation of equations (22), (23), (28), and (30); however, a link velocity independent, implementable form of the control law can easily be constructed in exactly the same manner as in [1]. That is, due to the fact that the control does not require measurement of $e_f(t)$, rather only functions of $e_f(t)$ (i.e., $Tanh(e_f)$, $Cosh^2(e_f)$, $Sinh(e_f)Cosh(e_f)$), we can make use of the following definition*

$$y_i = \tanh(e_{fi}) \tag{33}$$

*and standard relationships between hyperbolic functions to construct the following non-link-velocity dependent version for the filter given by (22)*

$$\begin{aligned} \dot{p}_i = & -(1-(p_i - ke_i)^2)(\alpha_3(p_i - ke_i) - \alpha_2 \tanh(e_i)) \\ & - k(\alpha_1 \tanh(e_i) + \alpha_2(p_i - ke_i)), \\ p_i(0) = & ke_i(0) \\ y_i = & p_i - k_{ei} \end{aligned} \tag{34}.$$

*As similarly illustrated in reference [1] for a different control law, the above filter and standard hyperbolic relationships can be utilized to remove link velocity measurements from the above control signals and the subsequently designed control signals as well. For example, we note that the adaptive update law given by (30) can be integrated by parts to obtain an implementable control signal for $\hat{\Phi}_v(t)$ that only depends on link position measurements (see reference [10])*

**3.2.2. Partial stability analysis for the robot and filter dynamics.** In this subsection, we present a partial stability analysis based on the dynamics given (21), (22), (30), and (31). This intermediate result will be used in the ensuing composite stability analysis of the closed-loop system. We begin the analysis by defining a non-negative, scalar function $V_1(t)$ as follows

$$\begin{aligned} V_1 = & \sum_{i=1}^{n} \Psi K_{mi}[\ln(\cosh(e_i)) + \ln(\cosh(e_{fi}))] \\ & + \frac{1}{2}\eta^T M(q)\eta + \frac{1}{2}\tilde{\Phi}_v^T K_{mx}\Gamma^{-1}\tilde{\Phi}_v. \end{aligned} \tag{35}$$

After taking the time derivative of (35), substituting (21), (22), (26), (29), (30), (31), and then cancelling common terms, making use of *Properties 2*, and *4*, and the fact that $\dot{\tilde{\Phi}}_v = -\dot{\hat{\Phi}}_v$, $\dot{V}_1(t)$ can be upper bounded by the following inequality

$$\begin{aligned} \dot{V}_1 \le & -\lambda_{\min}\{K_m\}\alpha_1\Psi\|Tanh(e)\|^2 + \eta^T K_m \eta_L - \alpha_2\|\eta\|^2 \\ & - \lambda_{\min}\{K_m\}\alpha_3\Psi\|Tanh(e_f)\|^2 + [\zeta_1\|x\|\,\|\eta\| \\ & - \alpha_2 k_{n1}\zeta_1^2\|\eta\|^2] \end{aligned} \tag{36}$$

where $\zeta_1$ and $k$ were defined in (26) and (29), respectively. After applying the nonlinear damping tool[17] to the bracketed terms in (36), a final upper bound can be placed on $\dot{V}_1(t)$ as follows

$$\begin{aligned} \dot{V}_1 \le & -\min\{\lambda_{\min}\{K_m\}\alpha_1\Psi,\ \lambda_{\min}\{K_m\}\alpha_3\Psi,\ \alpha_2\}\|x\|^2 \\ & + \frac{1}{\alpha_2 k_{n1}}\|x\|^2 + \eta^T K_m \eta_L \end{aligned} \tag{37}$$

where $x(t)$ was defined in (27). From the structure of (37), we are now motivated to design an actuator torque input control to drive $\eta_L(t)$ to zero.

### *3.3. Actuator torque input control design*

In this subsection*, we develop the actuator control torque input in a manner that ensures $\eta_L(t)$ is forced to zero. To this end, we present the development of a set of linear filters to compensate for the lack of actuator velocity measurements. At each step, a partial stability analysis is presented to motivate the control design procedure.

**3.3.1. Actuator velocity filter design.** From the actuator dynamics given in (1), we obtain the following expression

$$\ddot{q}_m = J^{-1}(u - B\dot{q}_m - K_m(q_m - q)). \tag{38}$$

Motivated by the need to formulate a surrogate expression for $\dot{q}_m(t)$, the auxiliary state variables $r_1(t)$, $r_2(t) \in \Re^n$ are defined as follows

$$\begin{bmatrix} r_1 \\ r_2 \end{bmatrix} = \begin{bmatrix} q_m \\ \dot{r}_1 + J^{-1}Br_1 \end{bmatrix}. \tag{39}$$

After taking the time derivative of $r_2(t)$ and then substituting (38) and (39), we have

$$\dot{r}_2 = J^{-1}u - J^{-1}K_m(r_1 - q). \tag{40}$$

In order to rewrite the actuator subsystem in a convenient state space form, we combine the time derivative of $r_1(t)$ of (39) with the expression given by (40) to yield

* Although the actuator velocity filter design is very similar to that of reference [19], we present the full development here for completeness of the paper, in addition to some notational differences.

https://doi.org/10.1017/S0263574799002167 Published online by Cambridge University Press

$$\begin{bmatrix} \dot{r}_1 \\ \dot{r}_2 \end{bmatrix} = A_0 r + \begin{bmatrix} k_{f1} I_n \\ k_{f2} I_n \end{bmatrix} r_1 + A_1 \begin{bmatrix} r_1 \\ 0_n \end{bmatrix} + A_2 \begin{bmatrix} 0_n \\ r_1 - q \end{bmatrix} + \begin{bmatrix} 0_n \\ J^{-1} u \end{bmatrix} \tag{41}$$

where $k_{f1}$, $k_{f2} \in \Re^1$ are constant, positive filter gains, the auxiliary matrices $A_0$, $A_1$, $A_2 \in \Re^{2n \times 2n}$ are defined as follows

$$A_0 = \begin{bmatrix} -k_{f1} I_n & I_n \\ -k_{f2} I_n & 0_{n \times n} \end{bmatrix}, \; A_1 = \begin{bmatrix} -J^{-1} B & 0_{n \times n} \\ 0_{n \times n} & -J^{-1} B \end{bmatrix} \tag{42}$$

$$A_2 = \begin{bmatrix} -J^{-1} K_m & 0_{n \times n} \\ 0_{n \times n} & -J^{-1} K_m \end{bmatrix}$$

$I_n \in \Re^{n \times n}$ represents the standard indentity matrix, $0_{n \times n}$ represents the zero matrix, and $0_n \in R^n$ represents the zero vector. From the definition of $k_{f1}$, $k_{f2}$, $J$, $B$, and $K_m$, it is straightforward to show that $A_0$, $A_1$, and $A_2$ are Hurwitz matrices.[18] Based on this fact and the form of (41), we follow the design procedure outlined in references [12] and [19] to formulate the following bounded-input, bounded-output, linear, actuator velocity independent filters

$$\begin{aligned} \dot{\varepsilon}_0 &= A_0 \varepsilon_0 + \begin{bmatrix} k_{f1} I_n \\ k_{f2} I_n \end{bmatrix} r_1 \quad \varepsilon_0 = [\varepsilon_{01} \;\; \varepsilon_{02}]^T \in \Re^{2n} \\ \dot{\varepsilon}_1 &= A_0 \varepsilon_1 + \begin{bmatrix} r_1 \\ 0_n \end{bmatrix} \qquad \varepsilon_1 = [\varepsilon_{11} \;\; \varepsilon_{12}] \in \Re^{2n} \\ \dot{\varepsilon}_2 &= A_0 \varepsilon_2 + \begin{bmatrix} 0_n \\ r_1 - q \end{bmatrix} \quad \varepsilon_2 = [\varepsilon_{21} \;\; \varepsilon_{22}]^T \in \Re^{2n} \\ \dot{\upsilon}_0 &= A_0 \upsilon_0 + \begin{bmatrix} 0 \\ u \end{bmatrix} \qquad \upsilon_0 = [\upsilon_{01} \;\; \upsilon_{02}]^T \in \Re^{2n}. \end{aligned} \tag{43}$$

Based on the structure of (43), we now design the state estimate for $r(t)$ as follows

$$\hat{r} = \varepsilon_0 + A_1 \varepsilon_1 + A_2 \varepsilon_2 + \begin{bmatrix} J^{-1} & 0_{n \times n} \\ 0_{n \times n} & J^{-1} \end{bmatrix} \upsilon_0. \tag{44}$$

From the definition of the parameter dependent state estimate for $r(t)$ given in (44), we define the state estimation error vector $\tilde{r}(t) \in R^{2n}$ as shown below

$$\tilde{r} = r - \hat{r} \tag{45}$$

where upon making the substitution for $\hat{r}(t)$ of (44) yields

$$\begin{bmatrix} \tilde{r}_1 \\ \tilde{r}_2 \end{bmatrix} = \begin{bmatrix} r_1 - \varepsilon_{01} + J^{-1}(B\varepsilon_{11} + K_m \varepsilon_{21} - \upsilon_{01}) \\ r_2 - \varepsilon_{02} + J^{-1}(B\varepsilon_{12} + K_m \varepsilon_{22} - \upsilon_{02}) \end{bmatrix}. \tag{46}$$

We now substitute (46) for $r_2(t)$ in (39) to obtain the surrogate expression for $\dot{q}_m(t)$ as follows

$$\dot{q}_m = \dot{r}_1 = \tilde{r}_2 + \varepsilon_{02} - J^{-1} B (q_m + \varepsilon_{12}) - J^{-1} K_m \varepsilon_{22} + J^{-1} \upsilon_{02}. \tag{47}$$

After examining (47), it is clear that we have separated the expression for the actuator velocity into i) measurable signals, ii) unknown parameters which will be adapted for in subsequent design, and iii) an unmeasurable signal (*i.e.*, $\tilde{r}_2(t)$) which will be forced to zero through the use of the nonlinear damping tool as shown in the subsequent stability analysis. Thus, the expression given by (47) will be used in lieu of $\dot{q}_m(t)$ during the ensuing stability analysis.

As an aid in the following stability analysis, we differentiate (46) with respect to time to obtain the following error system

$$\dot{\tilde{r}} = \dot{r} - \dot{\varepsilon}_0 - A_1 \dot{\varepsilon}_1 - A_2 \dot{\varepsilon}_2 + \begin{bmatrix} J^{-1} & 0_{n \times n} \\ 0_{n \times n} & J^{-1} \end{bmatrix} \dot{\upsilon}_0. \tag{48}$$

After substituting $\dot{r}(t)$ of (41) and the set of linear filters from (43) into (48), we can rewrite the dynamics for $\dot{\tilde{r}}(t)$ into the following convenient form

$$\dot{\tilde{r}} = A_0 \tilde{r}. \tag{49}$$

**3.3.2. Partial stability analysis for the actuator velocity filter.** We now present a partial stability analysis for the error system given by (49). Specifically, we define the non-negative, scalar function $V_2(t)$ as follows

$$V_2 = \tilde{r}^T P_0 \tilde{r} \tag{50}$$

where $P_0 \in \Re^{2n \times 2n}$ is a positive definite, symmetric, constant matrix, chosen such that

$$A_0^T P_0 + P_0 A_0 = -I_{2n}. \tag{51}$$

After taking the time derivative of (50), we have

$$\dot{V}_2 = \dot{\tilde{r}}^T \; P_0 \tilde{r} + \tilde{r}^T P_0 \; \dot{\tilde{r}}, \tag{52}$$

which after making substitutions for (49) and (51), reduces to the following expression

$$\dot{V}_2 = -\tilde{r}^T \tilde{r}. \tag{53}$$

From (53), it is straightforward task to upper bound $\dot{V}_2(t)$ as follows

$$\dot{V}_2 \leq -\|\tilde{r}_1\|^2 - \|\tilde{r}_2\|^2. \tag{54}$$

**3.3.3. Error system for the auxiliary tracking error signal $\eta_L$.** From the previous analysis of the link dynamics, we obtained motivation from (37) that illustrated that the signal $\eta_L(t)$ should be driven to zero. To calculate the dynamics for $\eta_L(t)$, we take the time derivative of (23), substitute (47) for $\dot{q}_m(t)$ and the time derivative of (28) for $\dot{q}_{md}(t)$, and then premultiply both sides of the resulting equation by $J$ to obtain

https://doi.org/10.1017/S0263574799002167 Published online by Cambridge University Press

$$J\dot{\eta}_L = J\left(\dot{Y}_{dx}\hat{\Phi}_v + Y_{dx}\dot{\hat{\Phi}}_v + \dot{q} - 2k\Psi Sinh^2(e_f)\dot{e}_f - k\Psi\dot{e}_f\right) + J(\Psi Cosh^{-2}(e)\dot{e} - \tilde{r}_2 - \varepsilon_{02}) + B(q_m + \varepsilon_{12}) + K_m\varepsilon_{22} - \upsilon_{02}. \quad (55)$$

Based on the structure of (55), we define the following linear parametrization

$$Y_L\theta_L = J\dot{Y}_{dx}\hat{\Phi}_v + J\dot{q}_d - J\varepsilon_{02} + B(q_m + \varepsilon_{12}) + K_m\varepsilon_{22} - J(\Psi Cosh^{-2}(e) - I_n)(\alpha_1 Tanh(e) + \alpha_2 Tanh(e_f)) - k\Psi J(2Sinh^2(e_f) + I_n)(\alpha_2 Tanh(e) - \alpha_3 Tanh(e_f)) \quad (56)$$

where $Y_L(e, e_f, \varepsilon_{02}, \varepsilon_{12}, \varepsilon_{22}, \hat{\Phi}_v, t) \in R^{n\times 3n}$ denotes a known regression matrix, and $\theta_L \in R^{3n}$ denotes an unknown constant parameter vector. After substituting (56) and (30) into (55), and then adding/subtracting an embedded control term $u_m(t) \in R^n$ to the right-hand side of the resulting equation, we have the following expression

$$J\dot{\eta}_L = Y_L\theta_L + J\Omega_1\eta - J\tilde{r}_2 + \eta_m - u_m \quad (57)$$

where the measurable auxiliary variable $\Omega_1(e, e_f, t) \in R^{n\times n}$ is defined as

$$\Omega_1 = Y_{dx}\Gamma Y_{dx}^T + \Psi Cosh^{-2}(e) - I_n + k^2\Psi Cosh^2(e_f)(2Sinh^2(e_f) + I_n), \quad (58)$$

and the auxiliary tracking error signal $\eta_m(t) \in R^n$, defined as follows

$$\eta_m = u_m - \upsilon_{02} \quad (59)$$

has been introduced to quantify how well the embedded control input $u_m(t)$ tracks the filter variable $\upsilon_{02}(t)$. Based on the previous development and the ensuing stability analysis, we design $u_m(t)$ in the following manner

$$u_m = k_L\eta_L + Y_L\hat{\theta}_L + k_{n2}\bar{K}_m^2\eta_L + k_{n3}\bar{J}^2\Omega_1^2\eta_L + k_{n4}\bar{J}^2\eta_L \quad (60)$$

where $k_L \in \Re^1$ is a constant scalar control gain, $k_{n2}$, $k_{n3}$, $k_{n4} \in \Re^1$ are constant scalar nonlinear damping gains, $\bar{J}$, $\bar{K}_m$ are defined in (13), and the update law for $\hat{\theta}_L(t) \in R^{3n}$ is given by

$$\dot{\hat{\theta}}_L = \Gamma_L Y_L^T\eta_L \quad (61)$$

with $\Gamma_L \in \Re^{3n\times 3n}$ being a positive definite, constant, diagonal, adaptation gain matrix. After substituting (60) into (57), we obtain the following closed-loop system for $\eta_L(t)$

$$J\dot{\eta}_L = Y_L\tilde{\theta}_L + \eta_m - k_L\eta_L + J\Omega_1\eta - J\tilde{r}_2 - k_{n2}\bar{K}_m^2\eta_L - k_{n3}\bar{J}^2\Omega_1^2\eta_L - k_{n4}\bar{J}^2\eta_L \quad (62)$$

where $\tilde{\theta}_L(t) \in \Re^{3n}$ is defined as follows

$$\tilde{\theta}_L = \theta_L - \hat{\theta}_L. \quad (63)$$

**3.3.4. Partial stability analysis for the auxiliary tracking error signal $\eta_L(t)$.** Continuing with the backstepping methodology, we now present a partial stability analysis for the error system given by (57). We begin by defining a non-negative, scalar function as follows

$$V_3 = \frac{1}{2}\eta_L^T J\eta_L + \frac{1}{2}\tilde{\theta}_L^T\Gamma_L^{-1}\tilde{\theta}_L. \quad (64)$$

After taking the time derivative of (64), substituting (61), (62), and using the fact that $\dot{\hat{\theta}}_L(t) = -\dot{\tilde{\theta}}_L(t)$, we can obtain the following upper bound for $\dot{V}_3(t)$

$$\dot{V}_3 \le \eta_L^T\eta_m - k_L\|\eta_L\|^2 - k_{n2}\bar{K}_m^2\|\eta_L\|^2 + [\bar{J}\|\Omega_1\|\,\|\eta_L^T\|\,\|\eta\| - k_{n3}\bar{J}^2\|\Omega_1\|^2\,\|\eta_L\|^2] + [\bar{J}\|\tilde{r}_2\|\,\|\eta_L\| - k_{n4}\bar{J}^2\,\|\eta_L\|^2]. \quad (65)$$

After applying the nonlinear damping tool [12] to the bracketed term in (65), we have

$$\dot{V}_3 \le -k_L\|\eta_L\|^2 - k_{n2}\bar{K}_m^2\|\eta_L\|^2 + \frac{\|\eta\|^2}{k_{n3}} + \frac{\|\tilde{r}_2\|^2}{k_{n4}} + \eta_L^T\eta_m. \quad (66)$$

**3.3.5 Error system for the auxiliary tracking error signal $\eta_m$.** From (66), we are motivated to continue the control design procedure to ensure that $\eta_m(t)$ is forced to zero. With this strategy in mind, we calculate the dynamics for $\eta_m(t)$ by taking the time derivative of $\eta_m(t)$ given in (59), and then substituting (43), (60), and (61) to obtain the following expression

$$\dot{\eta}_m = \dot{Y}_L\hat{\theta}_L + Y_L\Gamma_L Y_L^T\eta_L + 2k_{n3}\bar{J}^2\Omega_1\dot{\Omega}_1\eta_L + k_{f2}\upsilon_{01} - u + (k_L I_n + k_{n2}\bar{K}_m^2 I_n + k_{n3}\bar{J}^2\Omega_1^2 + k_{n4}\bar{J}^2 I_n)\dot{\eta}_L \quad (67)$$

where the terms $\dot{\eta}_L(t)$ and $\dot{\Omega}_1(t)$ can be calculated as follows

$$\dot{\eta}_L = J^{-1}Y_L\theta_L + \Omega_1\eta - \tilde{r}_2 - J^{-1}\upsilon_{02} \quad (68)$$

and

$$\dot{\Omega}_1 = 2Y_{dx}\Gamma\dot{Y}_{dx}^T + 2k^2\Psi Cosh(e_f)Sinh(e_f)\dot{e}_f(2Sinh^2(e_f) + 1) - 2\Psi Cosh^{-2}(e)Tanh(e)\dot{e} + 4k^2\Psi Cosh^3(e_f)Sinh(e_f)\dot{e}_f. \quad (69)$$

After substituting (68) and (69) into (67), we now write the dynamics for $\dot{\eta}_m(t)$ in the following advantageous form

$$\dot{\eta}_m = \Omega_2 + Y_f\theta_f + \Omega_3\eta + \Omega_4\tilde{r}_2 - u \quad (70)$$

where the known regression matrix $Y_f(\hat{B}, q_m, \varepsilon_{12}, \varepsilon_{22}, \upsilon_{02}, e, e_f, t) \in \Re^{n\times 3n}$, and the unknown constant vector $\theta_f \in \Re^{3n}$ are defined by the following linear parameterization

$$Y_f\theta_f = \hat{B}[-J^{-1}B(q_m + \varepsilon_{12}) - J^{-1}K_m\varepsilon_{22} + J^{-1}\upsilon_{02}] + [k_L I_n + k_{n2}\bar{K}_m^2 I_n + k_{n3}\bar{J}^2\Omega_1^2 + k_{n4}\bar{J}^2 I_n](J^{-1}B(q_m + \varepsilon_{12}) + J^{-1}K_m\varepsilon_{22} - J^{-1}\upsilon_{02}) \quad (71)$$

where the explicit expressions for the auxiliary terms $\Omega_2(t) \in \Re^n$, and $\Omega_3(t)$, $\Omega_4(t) \in \Re^{n\times n}$ are given in reference [20]. Motivated by the open loop error system for $\eta_m(t)$ given in (70) and the ensuing stability analysis, we now design the control torque input $u(t)$ as follows

$$u = k_m\eta_m + \Omega_2 + Y_f\hat{\theta}_f + k_{n5}\Omega_3^2\eta_m + k_{n6}\Omega_4^2\eta_m + \eta_L \quad (72)$$

where $\hat{\theta}_f(t) \in \Re^{3n}$ is updated via the following law

$$\dot{\hat{\theta}}_f = \Gamma_f Y_f^T\eta_m \quad (73)$$

$k_m \in \Re^1$ is a constant scalar control gain, $k_{n5}$, $k_{n6} \in \Re^1$ are constant scalar nonlinear damping gains, and $\Gamma_f \in \Re^{3n\times 3n}$ is a positive definite, constant, diagonal, adaptation gain matrix. After substituting the control torque input given by (72) into (70), we obtain the closed-loop system for $\eta_m(t)$ as shown below

https://doi.org/10.1017/S0263574799002167 Published online by Cambridge University Press

$$\dot{\eta}_m = Y_f\tilde{\theta}_f + \Omega_3\eta + \Omega_4\tilde{r}_2 - k_m\eta_m - k_{n5}\Omega_3^2\eta_m - k_{n6}\Omega_4^2\eta_m - \eta_L \quad (74)$$

where $\tilde{\theta}_f(t) \in \Re^{3n}$ is defined as follows

$$\tilde{\theta}_f = \theta_f - \hat{\theta}_f.$$

**3.3.6. Partial stability analysis for the auxiliary signal $\eta_m(t)$.** We begin the analysis by defining a non-negative, scalar function as follows

$$V_4 = \frac{1}{2}\eta_m^T\eta_m + \frac{1}{2}\tilde{\theta}_f^T\Gamma_f^{-1}\tilde{\theta}_f. \quad (75)$$

After taking the time derivative of (75), substituting (73) and (74), and then utilizing the fact that $\dot{\hat{\theta}}_f(t) = -\dot{\tilde{\theta}}_f(t)$, we have

$$\dot{V}_4 = \eta_m^T[\Omega_3\eta + \Omega_4\tilde{r}_2 - k_{n5}\Omega_3^2\eta_m - k_{n6}\Omega_4^2\eta_m] - \eta_m^T(k_m\eta_m + \eta_L) \quad (76)$$

which after the applying the nonlinear damping tool [12] to the bracketed terms, can be upper bounded as follows

$$\dot{V}_4 \le -k_m\|\eta_m\|^2 + \frac{\|\eta\|^2}{k_{n5}} + \frac{\|\tilde{r}_2\|^2}{k_{n6}} - \eta_m^T\eta_L. \quad (77)$$

## 4. MAIN RESULT

The closed-loop stability result and the appropriate conditions that guarantee global asymptotic link position tracking are developed in the following theorem.

**Theorem 1.** *Given the above control strategy, global asymptotic link position tracking is obtained in the sense that*

$$\lim_{t\to\infty} e(t) = 0 \quad (78)$$

*provided the nonlinear damping gains are selected to satisfy the following condition*

$$\min\{\lambda_{\min}\{K_m\}\alpha_1\Psi,\ \lambda_{\min}\{K_m\}\alpha_3\Psi,\ \alpha_2,\ 1,\ k_L,\ k_m\} > \frac{1}{\alpha_2 k_{n1}} + \sum_{i=2}^{6}\frac{1}{k_{ni}}. \quad (79)$$

**Proof**.We begin the proof of Theorem 1 by making use of (35), (50), (64), and (75) to construct the following non-negative, scalar function

$$V = \sum_{k=1}^{4} V_k. \quad (80)$$

After taking the time derivative of (80), substituting (37), (54), (66), and (77), and then simplifying the resulting expression, we obtain the following inequality

$$\dot{V} \le -\min\{\lambda_{\min}\{K_m\}\alpha_1\Psi,\ \lambda_{\min}\{K_m\}\alpha_3\Psi,\ \alpha_2\}\|x\| - \|\tilde{r}_1\|^2 - \|\tilde{r}_2\|^2 - k_L\|\eta_L\|^2 - k_m\|\eta_m\|^2 + \frac{\|x\|^2}{\alpha_2 k_{n1}} + \frac{\|x\|^2}{k_{n2}} + \frac{\|x\|^2}{k_{n3}} + \frac{\|\tilde{r}_2\|^2}{k_{n4}} + \frac{\|x\|^2}{k_{n5}} + \frac{\|\tilde{r}_2\|^2}{k_{n6}}. \quad (81)$$

The expression given by (81) can be further upper bounded as follows

$$\dot{V} \le -\left(\min\{\lambda_{\min}\{K_m\}\alpha_1\Psi,\ \lambda_{\min}\{K_m\}\alpha_3\Psi,\ \alpha_2,\ 1,\ k_L,\ k_m\} - \frac{1}{\alpha_2 k_{n1}} - \sum_{i=2}^{6}\frac{1}{k_{ni}}\right)\|z\|^2 \quad (82)$$

where $z(t) \in \Re^{7n}$ is defined as follows

$$z = [\,x^T \quad \tilde{r}_1^T \quad \tilde{r}_2^T \quad \eta_L^T \quad \eta_m^T\,]^T. \quad (83)$$

If the gain condition given in (79) is satisfied, then (82) can be expressed as the following negative semi-definite function

$$\dot{V} \le -\beta\|z\|^2 \quad (84)$$

where $\beta$ is some positive bounding constant.

Based on the properties of $\ln(\cosh(\cdot))$ and the manner that $V(t)$ given in (80) was defined, we can easily see that $V(t)$ is a radially unbounded, globally positive-definite function for all $e(t)$, $e_f(t)$, $\eta(t)$, $\eta_L(t)$, $\eta_m(t)$, $\tilde{r}_1(t)$, $\tilde{r}_2(t)$, $\tilde{\Phi}_v(t)$, $\tilde{\theta}_L(t)$ $\tilde{\theta}_f(t)$, and $t$. From (84), we can see that $\dot{V}(t)$ is negative semi-definite; hence, $V(t) \in L_\infty$. Since, $e(t)$, $e_f(t)$, $\eta(t)$, $\eta_L(t)$, $\eta_m(t)$, $\tilde{r}_1(t)$, $\tilde{r}_2(t)$, $\tilde{\Phi}_v(t)$, $\tilde{\theta}_L(t)$, and $\tilde{\theta}_f(t)$ are bounded for all time. From this fact and the assumptions on the desired link position trajectory, standard signal chasing arguments can be used to show that all signals in the RLFJ system and the proposed controller remain bounded for all time; hence, we can utilize (21), (22), (31), (62), and (74), to state that $\dot{e}(t)$, $\dot{e}_f(t)$, $\dot{\eta}(t)$, $\dot{\eta}_L(t)$, and $\dot{\eta}_m(t)$ are bounded for all time. Based on the preceding imformation, the definition of $z(t)$ in (83), and the structure of (84), we can conclude that $z(t)$, $\dot{z}(t) \in L_\infty^{7n}$ and that $z(t) \in L_2^{7n}$. Standard arguments can now be used [18] to show that $\lim_{t\to\infty} z(t) = 0$. Since $\lim_{t\to\infty} z(t) = 0$, we can utilize the definitions of $z(t)$ and $x(t)$ from (83) and (27), respectively, to conclude that $\lim_{t\to\infty} Tanh(e(t)) = 0$. The properties of the hyperbolic tangent function directly lead to the results given by (78).□

## 5. ADAPTIVE OUTPUT FEEDBACK EXTENSION

Provided exact model knowledge of the actuator dynamics is available, we can modify the adaptive PSFB design presented above to develop a global asymptotic link position tracking controller that adapts for parametric uncertainty in the link dynamics while only requiring link position measurements. To foster the development of a control torque input that is independent of actuator measurements, we utilize an actuator state observer.

### *5.1. Actuator state observer design*

To facilitate the development of an observer which obviates actuator position and actuator velocity measurements, we rearrange the actuator dynamics of (1) into the following state space form

https://doi.org/10.1017/S0263574799002167 Published online by Cambridge University Press

$$\begin{bmatrix} \dot{x}_1 \\ \dot{x}_2 \end{bmatrix} = \begin{bmatrix} x_2 \\ J^{-1}K_m(q - x_1) - J^{-1}Bx_2 + J^{-1}u \end{bmatrix} \quad (85)$$

where $x_1(t) = q_m(t) \in R^n$, and $x_2(t) = \dot{q}_m(t) \in R^n$. Based on the structure of (85), we construct the following state observer

$$\dot{\varrho} = \hat{x}_2 - K_m(Tanh(e) + Tanh(e_f)) \quad (86)$$

$$\dot{\hat{x}}_2 = J^{-1}K_m(q - \hat{x}_1) - J^{-1}B\hat{x}_2 + J^{-1}u \quad (87)$$

$$\hat{x}_1 = \varrho - K_m e \quad (88)$$

where $\hat{x}_1(t)$, $\hat{x}_2(t) \in R^n$ denote the estimates of the actuator position and velocity, respectively, and $\varrho(t) \in R^n$ is an auxiliary variable which allows the observer to be implemented without actuator measurements.

**5.2 Control torque input design and stability result.** Based on the control design for the link dynamics given in link (21), (22), (28), (29), (30), and the actuator state observer design given in (86), (87), and (88), we can construct the control torque input as follows

$$u_i = J_{ii}k_s\eta_{ai} + J_{ii}\Omega_{3i}(q, e, e_f, \eta_L, \eta_a, t) + J_{ii}\eta_{Li} + J_{ii}nk_{n8}\sum_{j=1}^{n}\Omega_{4ij}^2(q, e, e_f, \eta_L, t)\eta_{ai} - K_{mii}(q_i - \hat{x}_{1i}) + B_{ii}\hat{x}_{2i} \quad (89)$$

where $\eta_a(t) \in R^n$ denotes the actuator velocity tracking error defined as follows

$$\eta_a = x_{2d} - \hat{x}_2 \quad (90)$$

$x_{2d}(t) \in R^n$ denotes the desired actuator velocity designed as

$$x_{2di} = k_s\eta_{Li} + nk_{n7}\sum_{j=1}^{n}(\Omega_{2ij}(q, e, e_f, t) + 2K_{fij})^2\eta_{ai} + \Omega_{1i}(q, e, e_f, t) \quad (91)$$

$\eta_L(t)$ was defined in (23), the auxiliary terms denoted by $\Omega_1(q, e, e_f, t)$, $\Omega_2(q, e, e_f, t)$, $\Omega_3(q, e, e_f, \eta_L, \eta_a, t)$, and $\Omega_4(q, e, e_f, \eta_L, t)$ are obtained as shown below

$$\dot{q}_{md} = \Omega_1(q, e, e_f, t) + \Omega_2(q, e, e_f, t)\eta \quad (92)$$

$$\dot{x}_{2di} = \Omega_{3i}(q, e, e_f, \eta_L, \eta_b, t) + \sum_{j=1}^{n}\Omega_{4ij}(q, e, e_f, \eta_L, t)\eta_j \quad (93)$$

and $k_{n7}$, $k_{n8}$, $k_s \in R^1$ are positive constant control gains.

We can now define a non-negative, scalar function $V_5(t)$ as follows

$$V_5 = V_1 + \tfrac{1}{2}\tilde{x}_1^T\tilde{x}_1 + \tfrac{1}{2}\tilde{x}_2^TK_m^{-1}J\tilde{x}_2 + \tfrac{1}{2}\eta_a^T\eta_a + \tfrac{1}{2}\eta_L^T\eta_L \quad (94)$$

where $\tilde{x}_1(t)$, $\tilde{x}_2(t) \in R^n$ are defined as

$$\tilde{x}_1 = x_1 - \hat{x}_1 \quad \tilde{x}_2 = x_2 - \hat{x}_2 \quad (95)$$

and $V_1(t)$ was defined in (35), to prove that all closed-loop signals remain bounded for all time, and that the control torque input yields global asymptotic link position tracking as shown below

$$\lim_{t\to\infty} e(t) = 0 \quad (96)$$

provided that

$$\min\{\alpha_1\Psi\lambda_{\min}\{K_m\}, \alpha_3\Psi\lambda_{\min}\{K_m\}, \alpha_2, k_s\} > \tfrac{1}{\alpha_2 k_{n1}} + \tfrac{1}{k_{n7}} + \tfrac{1}{k_{n8}}. \quad (97)$$

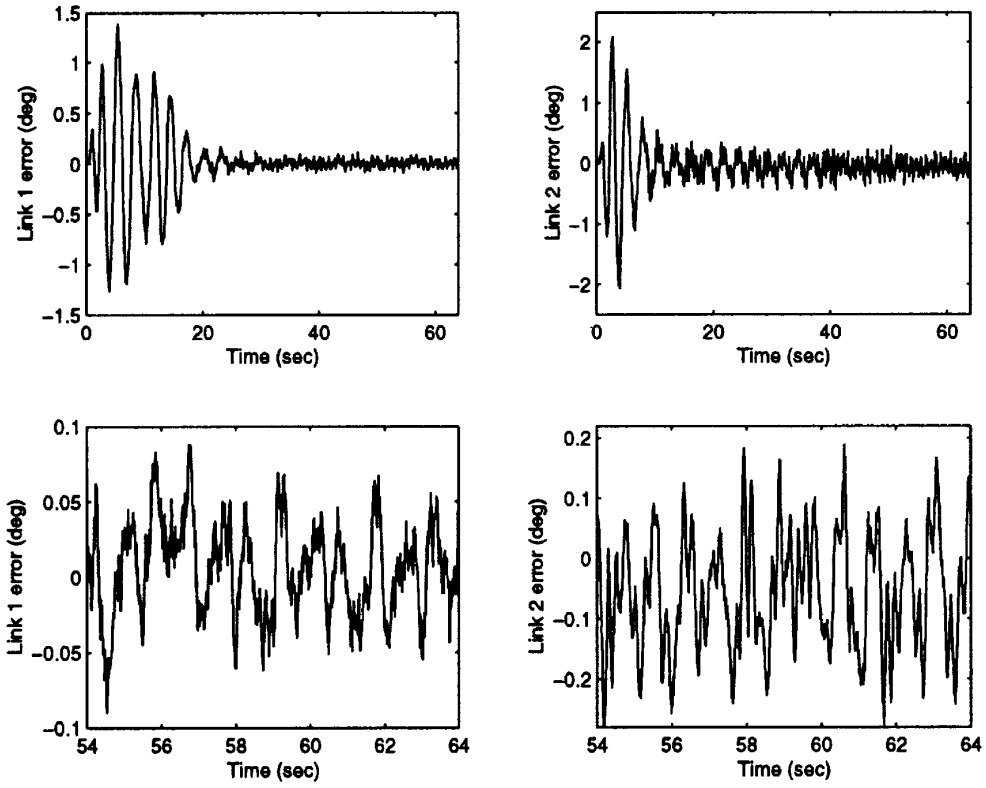


Fig. 1. Link position tracking errors.

https://doi.org/10.1017/S0263574799002167 Published online by Cambridge University Press

Table I. Comparison of Link Position Tracking Performance

| | Proposed Controller | PSFB-EMK controller [21] |
|---|---|---|
| Desired Trajectory (rad) | 1.0 sin (2.5$t$ (1 − $e^{-0.01t^4}$)) | 1.0 sin (2.4$t$ (1 − $e^{-0.01t^4}$)) |
| Spring Constant | Link 1: 150<br>Link 2: 18 | Link 1: 363<br>Link 2: 22 |
| Maximum Steady-State Tracking Error (deg.) | Link 1: 0.09<br>Link 2: 0.25 | Link 1: 0.22<br>Link 2: 0.20 |
| Maximum Required Torque (Nm) | Link 1: 40.0<br>Link 2: 3.5 | Link 1: 40.0<br>Link 2: 5.0 |

## 6. EXPERIMENTAL VERIFICATION

The proposed controller was implemented on a modified 2-link, revolute, direct-drive robot manipulator manufactured by Integrated Motion Inc. The robot modifications* include the addition of a new hub to decouple the link actuator from its respective link, and a pair of linear extension springs that serve as a new coupling between the actuator and the link. The actuator positions were measured with the built-in NSK resolvers, and the link positions were measured by 2 BEI 5000 line encoders. The links of the manipulator are actuated by switched-reluctance motors which are controlled through NSK torque controlled amplifiers. A Pentium 266 MHz PC operating under QNX (a real-time micro-kernal based operating system) hosts the control program. The control program was written in "C", and implemented using Qmotor 2.0, a Clemson University in-house graphical user interface. Data acquisition and control implementation were performed at a frequency of 2.5 kHz using the MultiQ I/O board. The dynamics of (1) for the experimental RLFJ robot manipulator can be characterized as follows

$$M(q) = \begin{bmatrix} 5.68 + 0.2C_2 & 0.43 + 0.01C_2 \\ 0.43 + 0.01C_2 & 0.43 \end{bmatrix} kg \cdot m^2/rad,$$

$$V_m(q, \dot{q}) = \begin{bmatrix} -0.10 s_2 \dot{q}_2 & -0.10 s_2 (\dot{q}_1 + \dot{q}_2) \\ 0.10 s_2 \dot{q}_1 & 0 \end{bmatrix} Nm \cdot sec/rad,$$

$$F_d = diag\{0.7, \quad 0.10\} Nm \cdot sec/rad,$$
$$K_m = diag\{150, \quad 18\} Nm/rad,$$

$$J = diag\{2.5 \quad 0.20\} kg \cdot m^2/rad,$$
$$B = diag\{1.3, 0.8\} Nm \cdot sec/rad$$

where $c_2$ denotes cos($q_2$) and $s_2$ denotes sin($q_2$).

The desired trajectory for links 1 and 2 were selected as the following *smooth-start* sinusoid

$$q_{d1} = q_{d2} = 1.0 \ \sin\left(2.5t\left(1 - e^{-0.01t^4}\right)\right) rad. \qquad (98)$$

The controller was tuned with the adaptation gains set to zero, and all of the initial adaptive estimates set to zero. The feedback, nonlinear filter, and the nonlinear damping gains were adjusted to reduce the link position tracking error. At

* A more in-depth description of the mechanical modifications to the IMI direct drive robot, including a schematic depiction, and photo of the modifications, can be found in [21].

Table II. Gain values for experimental varrification of PSFB RLFJ robot manipulator

| | Link 1 | | Link 2 | |
|---|---|---|---|---|
| control gains | $k_1 = 3.05$ $k_{L1} = 40$ $k_{m1} = 67$ | | $k_2 = 1.625$ $k_{L2} = 7$ $k_{m2} = 40$ | |
| filter gains | $\Psi_1 = 1.3$ $k_{f1} = 1$ | | $\Psi_1 = 1.85$ $k_{f2} = 5$ | |
| parameter update gains | $\Gamma_1 = 0.19$<br>$\Gamma_3 = 0.001$<br>$\Gamma_5 = 0$<br>$\Gamma_7 = 0$<br>$\Gamma_{L1} = 3.1$<br>$\Gamma_{L5} = 55$<br>$\Gamma_{m1} = 0.0005$<br>$\Gamma_{m5} = 5.0 \times 10^{-5}$ | $\Gamma_2 = 0.04$<br>$\Gamma_4 = 0.31$<br>$\Gamma_6 = 0.10$<br>$\Gamma_{L3} = 6.4$<br>$\Gamma_{m3} = 0.06$ | $\Gamma_8 = 0$<br>$\Gamma_{10} = 0.002$<br>$\Gamma_{12} = 0.05$<br>$\Gamma_{14} = 0.01$<br>$\Gamma_{L2} = 0.5$<br>$\Gamma_{L6} = 25$<br>$\Gamma_{m2} = 1.0 \times 10^{-5}$<br>$\Gamma_{m6} = 1.0 \times 10^{-6}$ | $\Gamma_9 = 0.01$<br>$\Gamma_{11} = 0$<br>$\Gamma_{13} = 0$<br>$\Gamma_{L4} = 2$<br>$\Gamma_{m4} = 1.0 \times 10^{-6}$ |

| | |
|---|---|
| nonlinear damping gains | $k_{n2} = 0.0015$, $k_{n3} = 1.0 \times 10^{-6}$, $k_{n4} = 5.0 \times 10^{-6}$, $k_{n5} = 7.5 \times 10^{-5}$, $k_{n6} = 1.0 \times 10^{-4}$ |
| filter gains | $\alpha_1 = 1.7$, $\alpha_2 = 0.6$, $\alpha_3 = 1.25$ |

https://doi.org/10.1017/S0263574799002167 Published online by Cambridge University Press

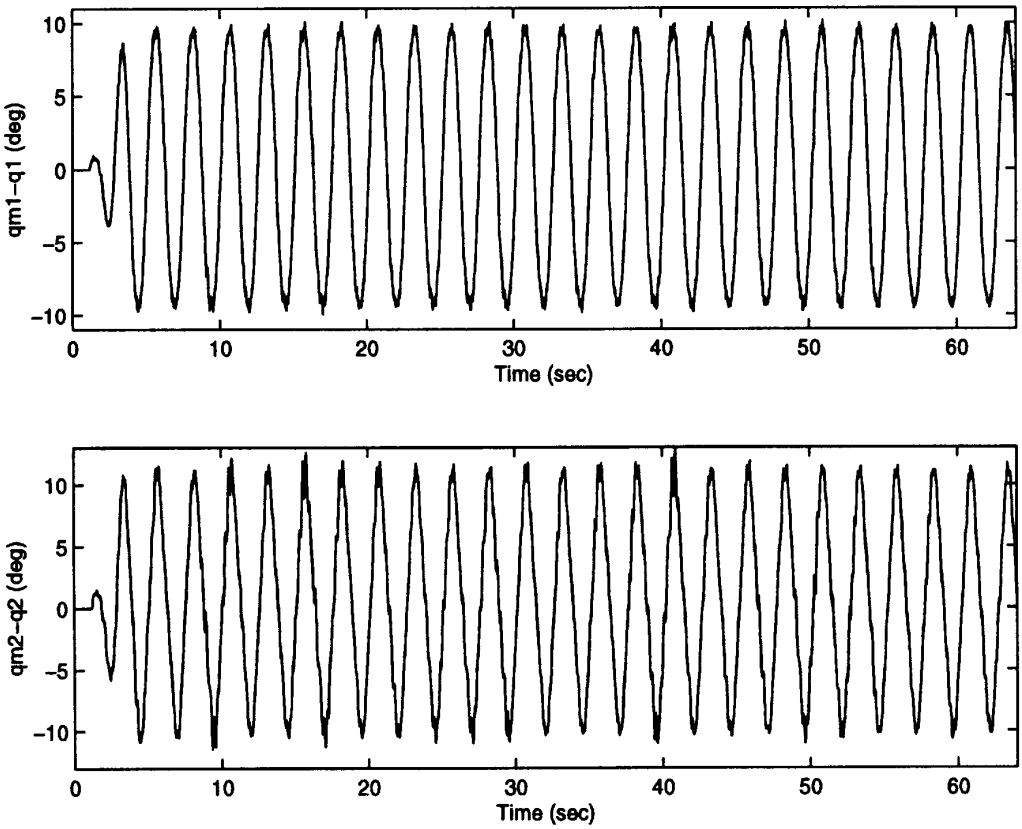


Fig. 2. Actuator/Link deflection.

some point, we noted that improved link position tracking error response could not be attained by adjustments of these controller gains. We then adjusted the adaptation gains to allow the parameter estimation to reduce the link position tracking error (see Figure 1 and Table I). After the tuning process was completed, the final gain values were recorded in Table II. The joint deflection for link 1 and link 2 is shown in Figure 2, the corresponding torque control inputs

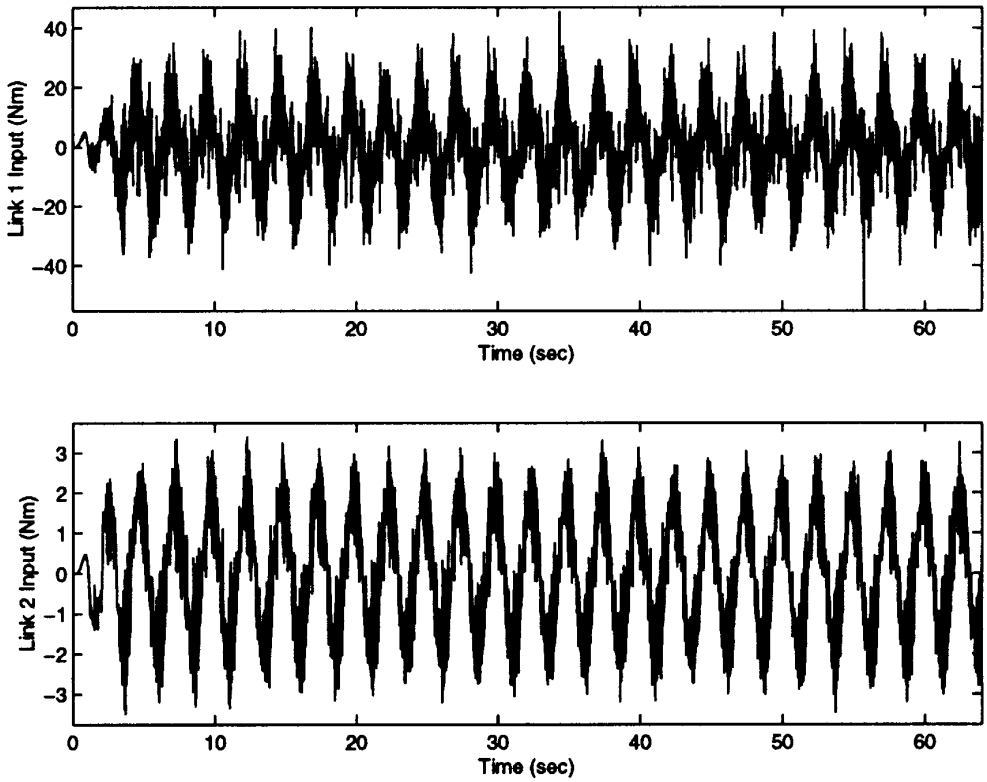


Fig. 3. Control torque input.

https://doi.org/10.1017/S0263574799002167 Published online by Cambridge University Press

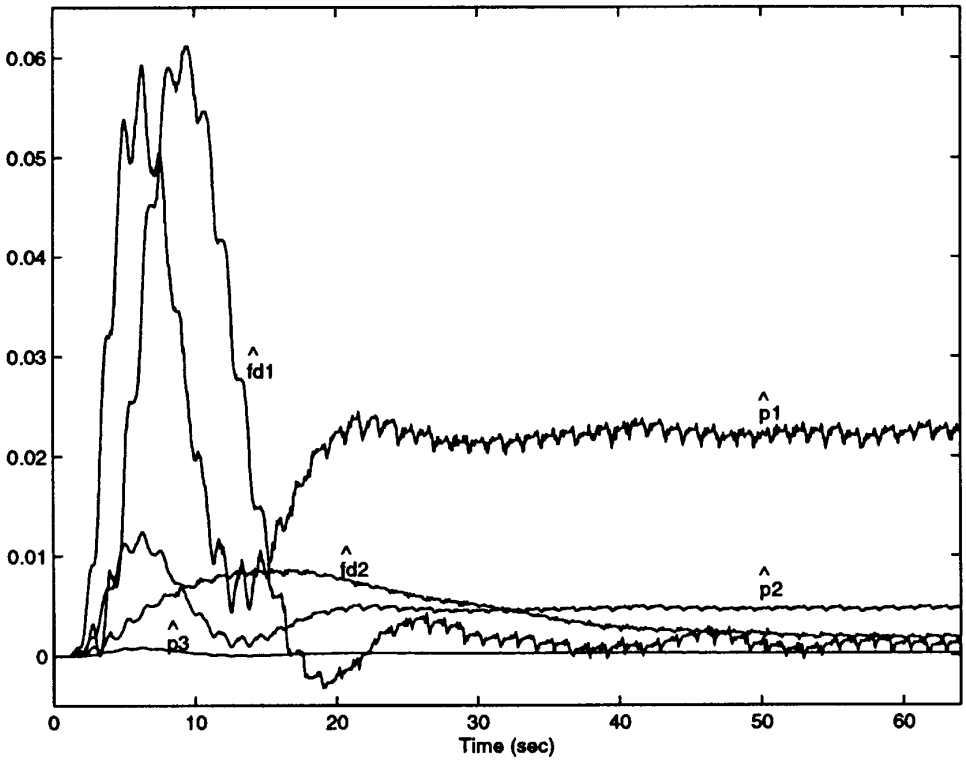


Fig. 4. Selected link dynamic parameter estimates.

are shown in Figure 3, and the parameter estimates shown in Figures 4, and 5.

**Remark 4.** *It is important to note, that due to the manner in which the expanded regression matrix was formed, there are several zero column vectors. As a result, we can set the corresponding adaptation gains (i.e.,* $\Gamma_5$, $\Gamma_7$, $\Gamma_8$, $\Gamma_{11}$, *and* $\Gamma_{13}$*) to zero for simplicity.*

**Remark 5.** *An experimental comparison between several simpler, reduced-order RLFJ control strategies and a complex full-order controller was given in [21]. Speci-*

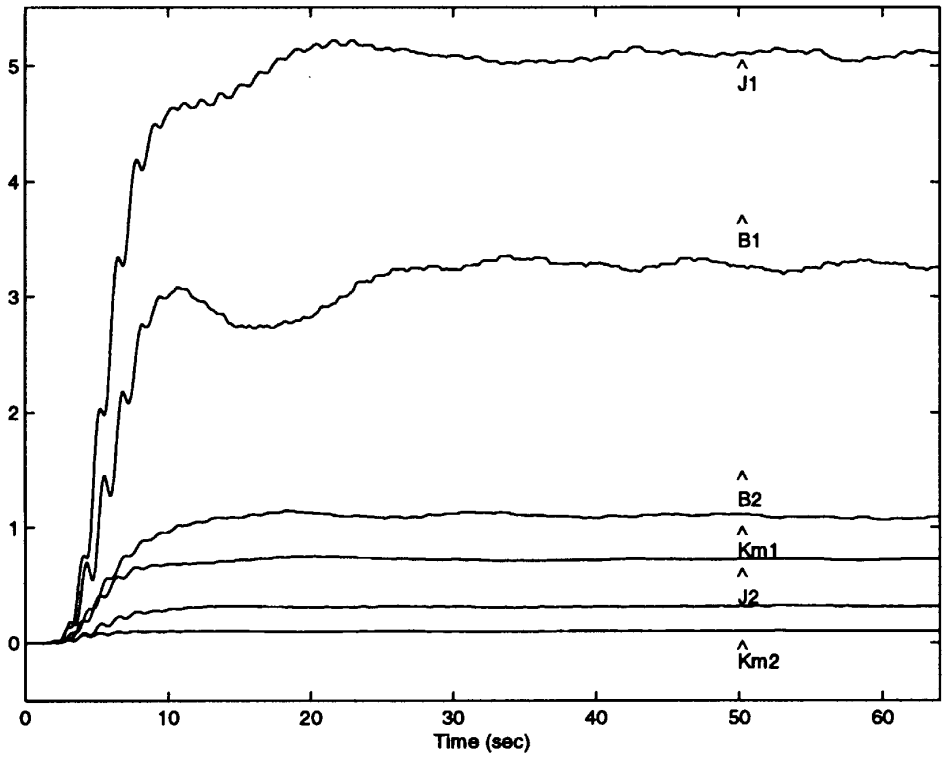


Fig. 5. Parameter estimates for the actuator dynamics.

https://doi.org/10.1017/S0263574799002167 Published online by Cambridge University Press

*fically, the full-order controller experimentally verified in [21] was an exact model knowledge, partial state feedback, link position tracking controller that required only link position and actuator position measurements and achieved semi-global link position tracking. The proposed controller represents a theoretical improvement over the full-order controller experimentally verified in [21] in that a global stability result is obtained (as opposed to semi-global), and that the proposed controller alleviates the need for exact model knowledge. That is, based on a comparison of the tracking performance of the two controllers (see Table I), we determine that despite 2.4 times more flexibility in the joint for Link 1, we are able to decrease the steady-state tracking error by 59%, for similar amplitude values of control torque. For the second link, we required 30% less control for a joint that is 1.2 times more flexible than in reference [21]; however 20% higher error was obtained.*

**Remark 6.** *We also noticed that the proposed controller was much easier to tune than the full-order controller experimentally verified in reference [21]. We attribute this change in tunability to the fact that the proposed controller is an adaptive controller, and hence, has some automatic tuning features (i.e., the adaptive update laws).*

## 7. CONCLUSIONS

In this paper, we have developed an adaptive, partial state feedback, link position tracking controller for rigid-link flexible-joint robots that exhibits global asymptotic link position tracking. Specifically, we utilize a nonlinear filter and a set of linear filters to remove the need for link and actuator velocity measurements. The controller compensates for parametric uncertainty throughout the entire mechanical system. A global output feedback extension was presented that adapts for parametric uncertainty in the link dynamics provided exact model knowledge of the actuator dynamics is available. Experimental results are given to illustrate the link position tracking performance of the proposed adaptive partial state feedback controller in comparison to an exact model knowledge partial state feedback controller.

## References


1. W.E. Dixon, E. Zergeroglu, D.M. Dawson and M.S. de Queiroz, "Global Output Feedback Tracking Control for Rigid-Link Flexible-Joint Robots", *Proc. of the International Conference on Robotics and Automation*, Leuven, Belgium (May 16–21, 1998) pp. 498–504.
2. P. Tomei, "A simple PD controller for Robots with Elastic Joints", *IEEE Transactions on Automatic Control* **36**, No. 10, 1208–1213 (Oct. 1991).
3. A. Ailon and R. Ortega, "An Observer-Based Set-Point Controller for Robot Manipulators with Flexible-Joints", *Systems and Control Letters* **21**, 329–335 (1993).
4. R. Kelly, R. Ortega, A. Ailon and A. Loria, "Global Regulation of Flexible-Joint Robots Using Approximate Differentiation", *IEEE Transactions on Automatic Control* **39**, No. 6, 1222–1224 (June 1994).
5. Z. Qu, "Input-Output Robust Tracking Control Design for Flexible-Joint Robots", *IEEE Transactions on Automatic Control* **40**, No. 1, 78–83 (Jan. 1995).
6. S. Nicosia and P. Tomei, "A Tracking Controller for Flexible-Joint Robots Using Using Only Link Position Feedback", *IEEE Transactions on Automatic Control* **40**, No. 5, 885–890 (May 1995).
7. S.Y. Lim, J. Hu, D.M. Dawson and M. Queiroz, "A Partial State Feedback Controller for Trajectory Tracking of Rigid-Link Flexible-Joint Robots Using an Observed Backstepping Approach", *J. Robotic Systems* **12**, No. 11, 727–746 (1995).
8. S.Y. Lim, D.M. Dawson, J. Hu and M.S de Queiroz, "An Adaptive Link Position Tracking Controller for Rigid-Link Flexible-Joint Robots Without Velocity Measurements", *IEEE Transactions on Systems, Man, and Cybernetics* **27**, No. 3, 412–427 (June 1997).
9. A. Loria, "Global Tracking Control of One Degree of Freedom Euler-Lagrange Systems Without Velocity Measurements", *European Journal of Control* **2**, No. 2, 144–151 (June 1996); see also *IFAC World Congress*, San Francisco, CA (July, 1996) **Vol. E**, pp. 419–424.
10. F. Zhang, D.M. Dawson, M.S de Queiroz and W.E. Dixon, "Global Adaptive Output Feedback Control of Robot Manipulators", *Proc. IEEE Conf. Decision and Control*, San Diego, CA, (Dec. 1997) pp. 3634–3639.
11. W.E. Dixon, F. Zhang, D.M. Dawson, and A. Behal, "Global Robust Output Feedback Tracking Control of Robot Manipulators", *Proc. of the 1998 IEEE International Conference on Control Applications*, Trieste, Italy (Sept. 1–4, 1998) (to appear).
12. M. Kristic, I. Kanellakopoulos and P. Kokotovic, *Nonlinear and Adaptive Control Design*, New York: John Wiley and Sons, 1995)
13. M. Sprong, "Modeling and Control of Elastic Joint Robots", *J. Dynamic Systems, Measurement, and Control* **109**, 310–319 (Dec, 1987).
14. M. Sprong and M. Vidyasagar, *Robotic Dynamics and Control*, New York: John Wiley and Sons, 1989)
15. F. Lewis, C. Abdallah and D. Dawson, *Control of Robot Manipulators*, (Macmillan Publishing Co. (New York, 1993)
16. T. Burg, D. Dawson, J. Hu and M. de Queiroz, "An Adaptive Partial State Feedback Controller for RLED Robot Manipulators", *IEEE Transactions on Automatic Control* **41**, No. 7, 1024–1031 (July, 1996).
17. P. Kokotovic, "The Joy of Feedback: Nonlinear and Adaptive", *IEEE Control Systems Magazine* **12**, 7–17 (June 1992).
18. S. Sastry and M. Bodson, *Adaptive Control: Stability, Convergence, and Robustness*, (Prentice Hall Co., Englewood Cliffs, N.J., 1989)
19. S.Y. Lim, D.M. Dawson and K. Anderson, "Re-examining the Nicosia-Tomei Robot Observer-Controller from a Backstepping Perspective", *IEEE Trans. on Control Systems Technology* **4**, No. 3, 304–310 (May, 1996).
20. W.E. Dixon, E. Zergeroglu, D.M. Dawson and M.W. Hannan, "Global Adaptive Partial State Feedback Tracking Control of Rigid-Link Flexible-Joint Robots", *1999 IEEE/ASME International Conference on Advanced Intelligent Mechatronics*, Atlanta, Georgia (September, 1999) ,(to appear).
21. M.S. de Queiroz, S. Donepudi, T. Burg, and D.M. Dawson, "Model-Based Control of Rigid-Link Flexible-Joint Robots: An Experimental Evaluation", *Robotica* **16**, Part 1, 11–21 (1998).


https://doi.org/10.1017/S0263574799002167 Published online by Cambridge University Press